Int. J. Electrochem. Sci., 10 **(2015)** 4393 - 4404

International Journal of ELECTROCHEMICAL SCIENCE
www.electrochemsci.org

Relationship between Dissolved Oxygen and Corrosion Characterization of X80 Steel in Acidic Soil Simulated Solution

Shuaixing Wang[1,*], *Daoxin Liu*[1], *Nan Du*[2], *Qing Zhao*[2], *Shuyun Liu*[2], *Jinhua Xiao*[2]

[1] Institute of Corrosion and Protection, Northwestern Polytechnical University, Xi'an, 710072, P. R. China
[2] School of Material Science and Technology, Nanchang Hangkong University, Nanchang 330063, P. R. China
[*]E-mail: wsxxpg@126.com

Received: 25 January 2015 / *Accepted:* 4 March 2015 / *Published:* 23 March 2015

The relationship between dissolved oxygen (DO) and corrosion behavior of X80 steel in acidic soil simulated solution was studied by potentiodynamic polarization curves, electrochemical impedance spectroscopy (EIS), scanning Kelvin probe technique (SKP) and X-ray diffraction (XRD). Results showed that the presence of DO accelerated the cathodic process of corrosion for X80 steel in the acidic soil simulated solution. With the decrease of DO, $1/R_{ct}$ and i_{corr} decreased gradually, the corrosion rate of X80 steel reduced. The corrosion of X80 steel was controlled by the ionization reaction when the content of DO in solution was bigger than 1.90 ppm. However, the diffusion of oxygen dominated the corrosion process of X80 steel in simulated solution with 0.85 ppm DO, as demonstrated by the presence of cathodic limiting diffusive current and Warburg impedance. Besides, DO could affect the formation and composition of the corrosion product formed on X80 steel. In O_2-saturated solution, a homogeneous and compact corrosion product layer, γ-FeOOH and Fe_3O_4, formed on the surface of X80 steel. But the phase composition of corrosion product was γ-FeOOH, Fe_2O_3 and a few $FeCO_3$ when DO in solution was 0.85 ppm.

Keywords: X80 steel; acidic soil; Corrosion; Dissolved oxygen; Electrochemical impedance spectroscopy (EIS); Scanning Kelvin probe (SKP)

1. INTRODUCTION

Pipelines are the most preferred method for transporting large volumes of crude oil and natural gas over long distances. X80 steel is a low carbon and micro-alloyed steel, and has been used widely for building the gas transmission pipelines because of its high-intensity and high-toughness [1-2]. As buried pipelines, X80 steel will pass through different soils, such as alkaline soil, neutral soil and acidic soil. According to the USDA soil taxonomy [3], acid red soil is one of major soil types in eastern and southeastern China. In this area, the annual precipitation is 1600 ~ 1700 mm, the temperature is above 15°C in all year, the pH of soil is 3.90~4.50 [4], which are easy to result in the corrosion of pipeline steel [5-9]. As we all know, corrosion of steel in soils is an electrochemical process. Oxygen and proton ion (H^+) have been recognized as the most common cathodic depolarizers in corrosion process of steel in soils [10-12]. It has been found that the compaction of soil will affect the air permeability. The diffusion of oxygen through water-saturated red soil is slow [13], the contribution of oxygen reduction to corrosion of the steel in water-saturated red soil can be negligible. However, loose red soil has good permeability, and red clay soil is acidic, both the depolarization of oxygen and the contribution of H^+ to corrosion may need to be considered. Therefore, it is necessary to clarify the role of dissolved oxygen (DO) in the corrosion process of X80 steel in acidic red soil.

Recently, the role of DO on the corrosion of carbon steel and stainless steel has been studied extensively[14-19]. Beak WC [14] considered that DO plays a significant role on the composition of the corrosion film formed on carbon steel. Cáceres L [15,16] found that the oxygen reduction reaction on iron is a mixed mass transfer and charge transfer controlled process, the cathodic current is predominantly mass-transfer controlled and steadily decreases with corrosion time at high NaCl concentrations, whereas at low NaCl concentrations, the current is predominantly charge-transfer controlled and increases with corrosion time. Li Y et al [17,18] demonstrated that the cathodic process on Q235 carbon steel in O_2-saturated 3.5% NaCl solution contains dissolved oxygen reduction, iron oxides reduction and hydrogen evolution, the oxygen molecule adsorption is inhibited by the adsorption of chloride ion on Q235 steel, the rate of oxygen reduction reaction will decrease with the increase of the concentration of chloride ion. However, so far, investigations are still inadequate to fully understand the relationship between oxygen and the corrosion mechanism of steel. Especially, there is little work about the role of DO on the corrosion of X80 steel in acid soil environment.

In this work, the relationship between DO and the electrochemical corrosion behavior of X80 steel in acidic soil simulated solution was investigated by polarization curves, EIS and SKP. The effects of DO on the corrosion products were analyzed by three dimensional video microscope and XRD. The results from this study have the potential to be useful in understanding the corrosion mechanism and improving the general criteria of soil corrosion.

2. EXPERIMENTAL

2.1 Materials and solution

API-X80 pipeline steel was used for all the tests in this work. The chemical composition was (wt%): C 0.036, Si 0.197, Mn 1.771, P 0.012，Mo 0.184，Nb 0.110，Ti 0.019，Cr 0.223，Ni 0.278，Cu 0.220，Al 0.021 and Fe balance. The X80 steel was cut into squares of 10 mm× 10 mm to act as working electrode. Specimens were connected to wires using conductive silver paste and then mounted in epoxy resins. The exposed surface area of the specimen was $1 cm^2$. Before each experiment, specimens were sequentially wet-ground with 400, 800, and 1200 grit silicon carbide emery papers and subsequently degreased ultrasonically in acetone for 10 min. Then, they were rinsed in deionized water and dried in a stream of cool air.

Yingtan (28°15′ N, 116°55′ E) was a typically hilly region of acidic soil in southeast China. The acidic red soil is Ultisol according to the USDA soil taxonomy [3]. In this work, simulated Yingtan soil solution was used, whose chemical compositions is given in Table 1. The pH of the solution was adjusted to 4.5±0.2 using sulfuric acid (H_2SO_4). All solutions were prepared by mixing analytical grade reagents with deionized water. Ultra-high purity argon gas and oxygen gas (>99.99%) were charged into simulated solution to adjust the concentration of DO. The content of oxygen in solution was measured by STARTER 300D.

Table 1. Chemical composition of acidic soil (Yingtan soil) simulated solution

Compounds	NaCl	$CaCl_2$	$MgSO_4 \cdot 7H_2O$	Na_2SO_4	$NaHCO_3$	KNO_3
Concentration(g/L)	0.0468	0.0111	0.0197	0.0142	0.0151	0.0293

2.2 Electrochemical measurement

Potentiodynamic polarization and EIS measurements were conducted by Autolab PGSTAT 302N. Tests were carried out using a three-electrode electrochemical cell with a saturated calomel electrode (SCE) as a reference and a platinum sheet as the counter electrode. The electrochemical test system was mounted into an earthed Faraday cage to minimize interference from outside electrical signals. Tafel plots of the steel were measured potentiodynamically from -2.0 V to 1.0 V (vs. SCE) at a scan rate of 1 mV/s. The impedance spectra were acquired at open-circuit potential (OCP) over the frequency range of $10^5 \sim 10^{-2}$ Hz using an AC signal amplitude of 10 mV. The equivalent circuits were fitted using the Zsimpwin software. All tests were performed at room temperature (25 ± 2 °C).

All experiments were repeated by three duplicate specimens to confirm reproducibility of the results, and the typical result or the average of the three measurements was reported in this paper.

2.3 Surface characterization

The morphology of corroded X80 steel was obtained using a KH-7700 three dimensional video microscope. Besides, the surface potential of corroded X80 steels was measured by a SKP system (KP technology Ltd, UK) at room temperature in air. The scanning microprobe was made by gold. The distance between the probe tip and the specimen was maintained at 100 μm ± 10 μm throughout the tests, avoiding the potential fluctuation due to the change of the distance. The scanning step was 250 μm, the scanning area was 3 mm × 3mm. The phase composition of corrosion product on X80 steel was investigated by X-ray diffraction (XRD), using a Bruker D8-Advance instrument with ascan range from 20° to 80° (in 2θ).

3. RESULTS AND DISCUSSION

3.1 Concentration of DO in simulated solution

In this work, ultra-high purity argon gas and oxygen gas were used to adjust the concentration of DO in simulated solution. Fig.1 gives the relationship curves between aeration time and DO concentration. It can be seen that the content of DO in simulated solution was about 4.10 ppm under open system. The lowest content of DO could reduce to 0.85 ppm by inflating argon gas. Besides, the O_2-saturated simulated solution contained about 20.20 ppm DO. Accordingly, the electrochemical corrosion behavior of X80 steel in acidic soil simulated solution with DO of 0.85~ 20.20 ppm was analyzed.

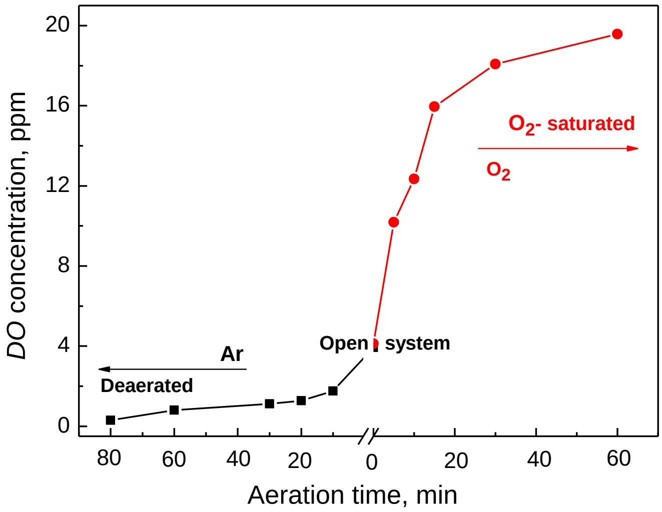

Figure 1. Relationship curve between aeration time and DO content in acidic soil simulated solution

3.2 Polarization behavior

Fig.2 presents the polarization curves of X80 steel in acidic soil simulated solutions with different level of DO. Correspondingly, the variation curves of i_{corr} and E_{corr} are given in Fig.3. It can be seen that X80 steel showed active behavior in O_2-saturated (DO 20.20 ppm) simulated solution. With the decrease of DO, the corrosion process of X80 steel inhibited, i_{corr} reduced greatly, E_{corr} moved negatively. Besides, X80 steel had the tendency of passivity as DO decreased. When DO was 0.85 ppm, there was limiting diffusive current and obvious passivity characteristics on the cathodic branch and anodic branch of polarization curve, respectively. Therefore, it can be inferred that the presence of oxygen accelerated the cathodic process of corrosion of X80 steel. In the simulated solution with higher level of DO, the corrosion of X80 steel was controlled by the electrochemical activation reaction. The diffusion of oxygen dominated the corrosion process of X80 steel in simulated solution with 0.85 ppm DO, as demonstrated by the presence of cathodic limiting diffusive current [21].

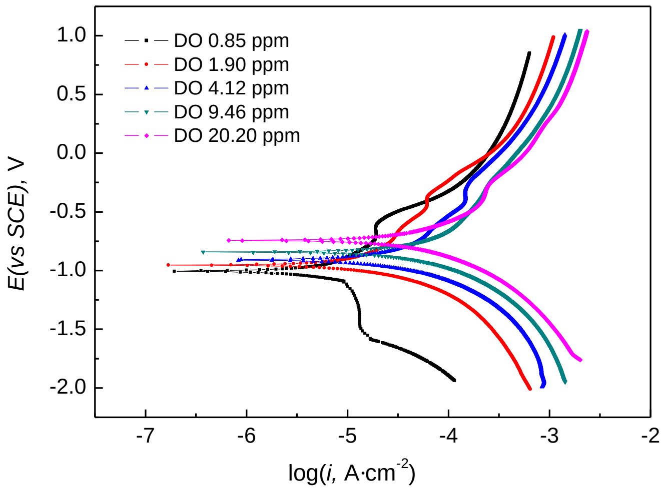

Figure 2. Polarization curves of X80 steel in acidic soil simulated solutions with different content of DO

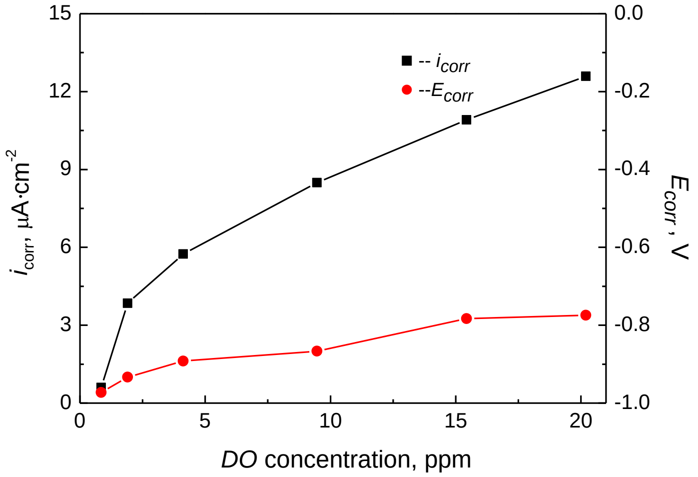

Figure 3. i_{corr} and E_{corr} of X80 steel in acidic soil simulated solutions with different content of DO

3.3 EIS behavior

EIS has been shown to be a powerful tool to obtain kinetic parameters of electrochemical reactions involved in corrosion processes [6, 22, 23] . Fig.4 gives the EIS plots for X80 steel immersed in acid soil simulated solutions with different level of DO. In O_2-saturated (DO 20.20 ppm) solution, EIS plot displayed a high-frequency loop and a depressed semicircular arc in the low frequency region. With the decrease of DO, the integrity of high-frequency loop reduced, the radius of low-frequency arc increased. However, the EIS plot had an obvious change when DO was 0.85 ppm, Warburg impedance appeared on the low-frequency region. Generally, the high-frequency loop is attributed to the response of deposited corrosion products [6,23]. The depressed low-frequency arc is associated with the corrosion process in the steel/solution interface. Whereas, Warburg impedance is the response of diffusion process for oxygen or corrosion products [24, 25]. Therefore, it could be confirmed that the corrosion of X80 steel was controlled by the ionization reaction when DO was bigger than 1.90 ppm, but the diffusion of oxygen dominated the corrosion of X80 steel when DO was 0.85 ppm. Besides, the resistance of corrosion reaction for X80 steel increased, the corrosion rate reduced, and the coverage degree of corrosion products showed a decreasing trend when DO decreased.

Equivalent electrical circuit in Fig. 5a can be used to characterize the EIS data when DO is 20.20 ~ 1.90 ppm. Where, R_s represents the electrolyte resistance; C_{dl} and R_{ct} pair in parallel characterizes the low frequency loop, C_{dl} is the double layer capacitance at the metal/solution interface, R_{ct} represents the charge transfer resistance; Q_f and R_f correspond to the non-ideal capacitance and resistance of corrosion product layer, respectively. In addition, there is Warburg impedance in EIS plot when DO is 0.85 ppm, so Z_W is used to represent the diffusion resistance of DO, as shown in Fig. 5b. Where, Q is a constant phase element, $Q = Y_0^{-1}/(j\omega)^n$, n is the frequency dispersion factor and varies from 1 to 0. $Z_W = (j\omega)^{-0.5} Y_w^{-1}$, Y_w is a constant, the smaller Y_w showed the bigger diffusion resistance of medium [25] . As shown in Fig.4, the equivalent circuits fitted the experimental data well, indicating that the equivalent circuits of Fig.5 were suitable.

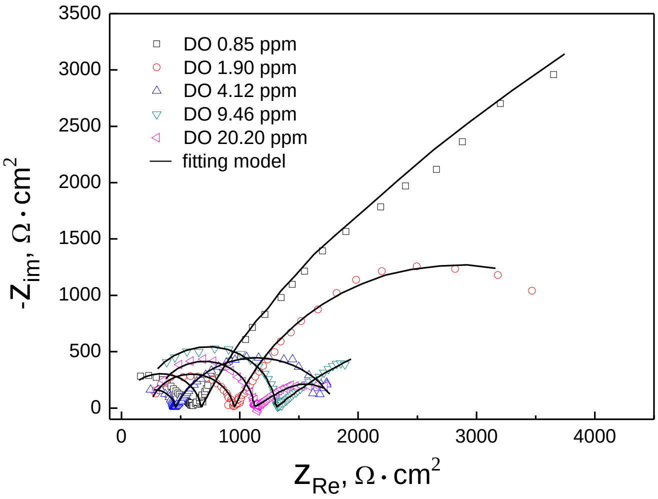

Figure 4. Nyqusit plots for X80 steel in acid soil simulated solutions with different content of DO

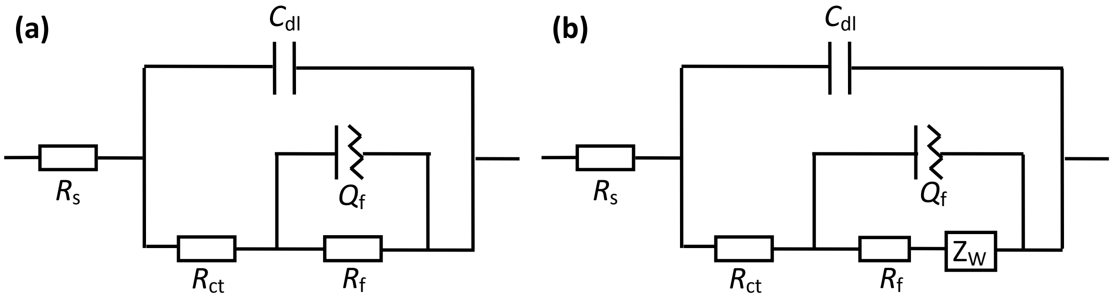

Figure 5. Equivalent circuits of EIS plots for X80 steel in acid soil simulated solutions with different content of DO (a) DO = 20.20 ~1.90 ppm, (b) DO = 0.85 ppm

Table 2. EIS component values for X80 steel in simulated solutions with different level of DO

DO content (ppm)	Electric components						
	R_{ct} ($\Omega\cdot cm^2$)	C_{dl} ($F\cdot cm^{-2}$)	n_{dl}	R_f ($\Omega\cdot cm^2$)	Q_f ($F\cdot cm^{-2}$)	n_f	Y_W ($\Omega^{-1}\cdot S^{1/2}\cdot cm^{-2}$)
20.20	463.5	1.677×10^{-9}	0.8756	483.7	7.744×10^{-4}	0.7343	—
9.46	539	5.074×10^{-8}	0.9697	461.4	3.934×10^{-3}	0.6605	—
4.12	667.2	1.582×10^{-8}	0.9219	289.1	1.577×10^{-3}	0.5181	—
1.90	918.1	6.592×10^{-8}	0.888	397.6	1.434×10^{-3}	0.6305	—
0.85	1176	1.405×10^{-8}	0.9371	327.4	1.144×10^{-3}	0.6087	4.351×10^{-4}

Table 2 shows the fitting component values for EIS. Generally, $1/R_{ct}$ is taken as a parameter to characterize the corrosion rate [24, 26, 27] , R_f and n_f can display the features of the corrosion products. Fig.6 and Fig.7 present the evolution of $1/R_{ct}$, R_f and n_f for X80 steel in simulated solution with different level of DO, respectively. As shown in Fig.6 and Fig.3, $1/R_{ct}$ had a similar variation rules with i_{corr}. In O_2-saturated solution, both $1/R_{ct}$ and R_f, n_f were significantly higher, which indicated that the corrosion of X80 steel occurred easily, but the surface of X80 steel could form compact corrosion product layer in this status. $1/R_{ct}$ decreased with the decrease of DO, which showed the corrosion rate of X80 steel reduced. Meanwhile, R_f and n_f decreased when DO changed from 20.20 ppm to 4.12 ppm, which showed that the corrosion product layer had poorer protection. However, R_f and n_f increased slightly when DO reduced from 4.12 ppm to 0.85 ppm, indicating that the coverage of corrosion product on X80 steel improved slightly. Besides, the low Y_w implied large diffusion resistance for DO when DO was 0.85 ppm.

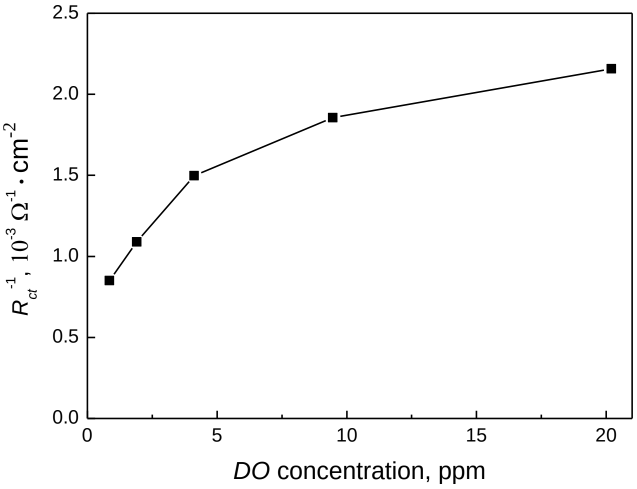

Figure 6. Evolution of $1/R_{ct}$ for X80 steel in acid soil simulated solution with different content of DO

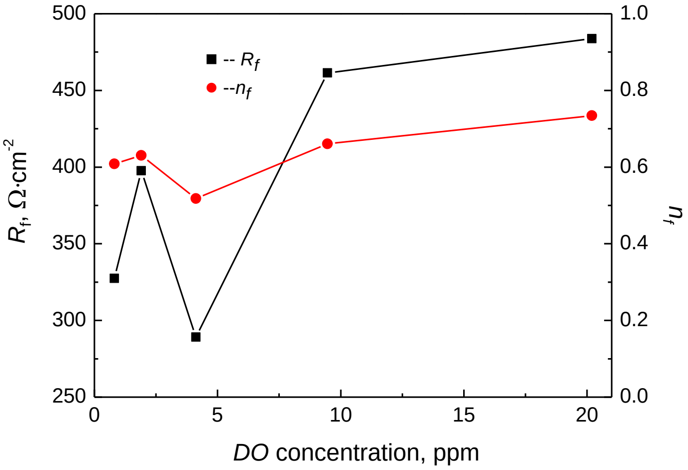

Figure 7. Evolution of R_f and n_f for X80 steel in acid soil simulated solution with different content of DO

3.4 Surface analysis

Scanning Kelvin probe (SKP) technique, a non-intrusive electrochemical method allowing the measurement of localized variation of potential in-situ over the surface of active material, has been used to research the corrosion behavior of materials in recent [21, 28, 29]. Fig.8 shows the OM image and SKP potential distribution of X80 steel with different status. It can be seen that the surface potential of un-corroded X80 steel was very negative, but the potential distribution was uniform. The surface of X80 steel was covered by the corrosion product after 48 h exposure in the simulated solution, regardless of the level of DO. In addition, the surface potential moved positively, the potential difference increased, and obvious cathodic regions and anodic regions appeared in the SKP map when X80 steel was immersed in simulated solution for 48 h. As shown in Fig.8d, the surface of X80 steel was almost completely covered by corrosion products when DO was 20.20 ppm. As for the X80 steel after corrosion in solution with 0.85ppm DO (Fig.8b), many clumpy corrosion products appeared on the surface, but the corrosion products cloud not effectively cover the surface. Moreover, there was only part of flaky corrosion products on X80 steel, the coverage of corrosion product was very low when DO was 4.12ppm, as shown in Fig.8c.

In addition, the surface morphology of corroded X80 steel and SKP potential distribution exhibited a good consistency, as shown in Fig.8. When DO was 20.20 ppm, the surface potential of X80 steel was more positive, the potential distribution was uniform, and the potential difference was only 98 mV, indicating that a homogeneous corrosion product layer was almost formed on the surface of X80 steel. When DO was 4.12 ppm, the surface potential of X80 steel was more negative and fluctuated significantly, the maximum of potential difference reached to 189 mV, the activity regions showed striated distribution, which indicated that a layer of loose, porous corrosion product might form on electrode surface, without changing the active dissolution state of the steel. In this status, the regions covered by corrosion products were micro-cathodes, the bare regions were micro-anodes, and so the electrochemical corrosion occurred easily. Furthermore, the surface potential of X80 steel was -

189mV~ -53mV, and there was a few of activity regions in the SKP distribution map when DO was 0.85 ppm. This result indicated that the corrosion product on X80 steel was relatively uniform, but the corrosion products cloud not cover the entire surface. Interestingly, the surface status of X80 steel analyzed by SKP distribution was consistent with the OM image and R_f fitted by EIS.

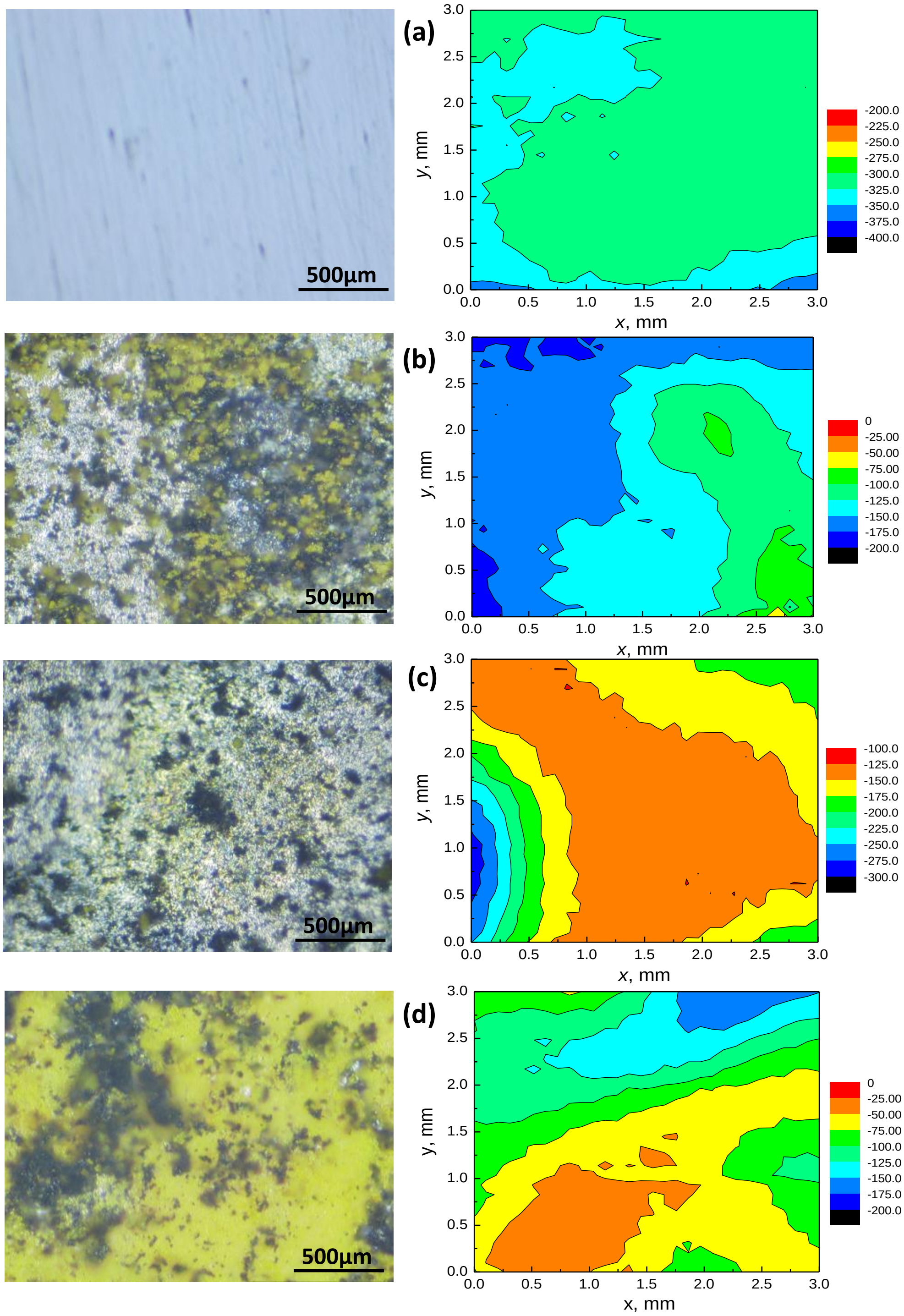

Figure 8. OM image (left) and SKP potential distribution (right) of un–corroded X80 steel (a) and X80 steel immersed in acid soil simulated solutions with 0.85 ppm DO (b), 4.12 ppm DO (c) and 20.20 ppm DO (d).

XRD patterns of corrosion product for X80 steel exposed in the simulated solution for 48 h are shown in Fig.9. The composition and content of corrosion product had significant differences when X80 steel was immersed in simulated solution with different level of DO. In O_2-saturated solution, the phase composition of corrosion product on X80 steel was mainly γ-FeOOH and Fe_3O_4. With the decrease of DO, the diffraction peak of Fe_3O_4 reduced gradually. When DO was reduced to 0.85 ppm, Fe_3O_4 was basically replaced by Fe_2O_3, meanwhile, a few $FeCO_3$ appeared on the corrosion product.

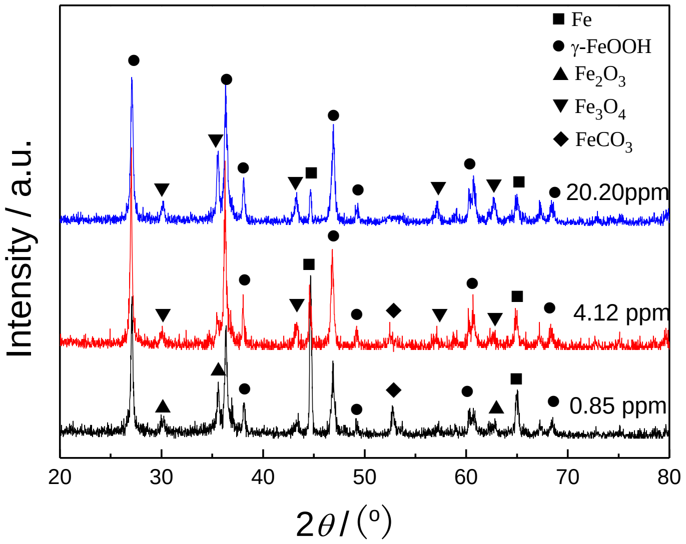

Figure 9. XRD pattern of corrosion product on X80 steel immersed in acid soil simulated solutions with different content of DO for 48h

3.5 Analysis of corrosion mechanism

Generally, corrosion of steel in soils is an electrochemical process. Oxygen and H^+ have been recognized as the most common cathodic depolarizers in corrosion process of steel. Related researches [5, 6, 8,26] had shown that the anodic process of corrosion of X80 steel was the dissolution of Fe (Eq.1), the cathodic reaction of corrosion was mainly the depolarization of oxygen (Eq.2) in the acid soil environment.

In the simulated solution with higher level of DO, the corrosion of X80 steel was governed by the electrochemical activation reaction. In O_2-saturated solution, the driving force of reduction reaction of oxygen was large, which resulted in the acceleration of the dissolution of Fe, and so the corrosion of X80 steel was serious in this status, as demonstrated by the bigger value of $1/R_{\mathrm{ct}}$ and i_{corr}. However, the sufficient DO in the solution could promote the transformation of corrosion product (see in Eq.3, Eq.4, Eq.5, Eq.6). In this system, a homogeneous and compact corrosion product layer, γ-FeOOH and Fe_3O_4, formed on the surface of X80 steel, as shown in Fig.8d and Fig.9. However, the formation and dissolution of corrosion product layer occurred alternately on the steel as the erosion effect of active ions (H^+, Cl^-, et al) in acidic soil simulated solution. Besides, γ-FeOOH and Fe_3O_4 may be reduction, so the passivity did not appear on the polarization curve when DO was 20.20 ppm.

With the decrease of DO, the transfer rate of oxygen could not meet the needs of cathodic process, the reduction of oxygen was inhibited, and the electronics formed by the dissolution of Fe (Eq.1) accumulated on the surface of steel electrode, which resulted in the decrease of E_{corr} of X80 steel. In addition, the weakening of depolarization reaction of oxygen made the anodic reaction slow down, so the corrosion rate of X80 steel reduced, as shown that $1/R_{\mathrm{ct}}$ and i_{corr} decreased gradually with the decrease of DO.

However, the diffusion of oxygen dominated the corrosion process of X80 steel in simulated solution with 0.85 ppm DO. It has been demonstrated that the diffusion way of oxygen to micro-cathode of steel electrode was similar with a cone, a few micro-cathodes might occupy all the diffusion path of oxygen [30]. When the level of DO was low, micro-cathodes of X80 steel might adsorb competitively the little oxygen in solution, which made the diffusion path of oxygen become longer, as demonstrated by the low Y_w. The DO arrived the micro-cathodes of steel by the diffusion decreased significantly, which made the depolarization effect of oxygen reduce, and so the anodic reaction was inhibited, the corrosion rate of X80 steel decreased. Besides, Fe^{2+} generated by the anodic process might react with HCO_3^- in solution and formed $FeCO_3$ (Eq.7) as the decrease of depolarization effect of oxygen. Moreover, Fe_2O_3 (Eq.8) became the main corrosion product in this status. Generally, the protective effect of $FeCO_3$ was better than that of FeOOH, the stability of Fe_2O_3 was also better, so X80 steel could be passive when DO was 0.85 ppm.

$$Fe-2e \rightarrow Fe^{2+} \quad (1)$$

$$O_2 + 4H^+ + 4e \rightarrow 2H_2O \quad (2)$$

$$Fe^{2+} + 2H_2O \rightarrow Fe(OH)_2 + 2H^+ \quad (3)$$

$$4Fe(OH)_2 + O_2 + 2H_2O \rightarrow 4Fe(OH)_3 \quad (4)$$

$$2Fe(OH)_3 + Fe(OH)_2 \rightarrow Fe_3O_4 + 4H_2O \quad (5)$$

$$Fe(OH)_3 - H_2O \rightarrow FeOOH \quad (6)$$

$$Fe^{2+} + HCO_3^- \rightarrow FeCO_3 + H^+ \quad (7)$$

$$4Fe(OH)_2 + O_2 \rightarrow 2Fe_2O_3 + 4H_2O \quad (8)$$

4. CONCLUSION

In the acidic soil simulated solution, the presence of DO accelerated the cathodic process of corrosion for X80 steel. In O_2-saturated solution (DO 20.20 ppm), the corrosion of X80 steel was governed by the ionization reaction. With the decrease of DO, $1/R_{\mathrm{ct}}$ and i_{corr} decreased gradually, the corrosion rate of X80 steel reduced. However, the diffusion of oxygen dominated the corrosion process of X80 steel in simulated solution with 0.85 ppm DO, as demonstrated by the presence of cathodic limiting diffusive current in polarization curve and Warburg impedance in EIS plot.

Furthermore, DO could affect the formation and composition of the corrosion product formed on X80 steel. In O_2-saturated solution, a homogeneous and compact corrosion product layer, γ-FeOOH and Fe_3O_4, formed on the surface of X80 steel. A layer of loose, porous corrosion product formed on steel surface when DO decreased. Otherwise, the phase composition of corrosion product was γ-FeOOH, Fe_2O_3 and a few $FeCO_3$ when X80 steel exposed in the simulated solution with 0.85 ppm DO.

ACKNOWLEDGEMENTS
We would like to express our appreciation to National Natural Science Foundation of China (Grant No. 51161021) for providing the financial support to this work.

References

1. A. V. Borovikov, *Metallurgist*, 47 (2003) 415-418.
2. J. Niu, L. H. Qi, Y. L. Liu, L. Ma, Y. R. Feng, J. X. Zhang, *Trans. Nonferrous. Met. Soc. China*, 19 (2009) 573-578.
3. S.S. Staff, Keys to Soil Taxonomy 11th ed., United States Department of Agriculture, Natural Resources Conservation Service, Washington, DC, 2010.
4. R. Xu, A. Zhao, Q. Li, X. Kong, G. Ji, *Geoderma*, 115 (2003) 75- 84.
5. B. Zhao, C. W. Du, Z. Y. Liu, X. G. Li, J. K. Yang, Y. Q. Li, *Acta Metall. Sin.*, 48 (2012) 1530-1536 (in Chinese).
6. L. Zhang, X. G. Li, C. W. Du, *J. Iron Steel Res. Int.*, 16 (2009) 52-57.
7. Z. Liu, X. Li, Y. Zhang, C. Du, *Acta Metall. Sin. (Engl. Lett.)*, 22 (2009) 58-64.
8. X. Chen, C. W. Du, X. G. Li, C. He, P. Liang, L. Lu, *Int. J. Miner. Metall. Mater.*, 103 (2007) 9-13.
9. Y.H. Wu, T.M. Liu, C. Sun, J. Xu, C.K. Yu, *Corros. Eng. Sci. Technol.*, 45 (2010) 136-141.
10. C.P. Gardiner, R.E. Melchers, *Corros. Sci.*, 44 (2002) 2665-2673.
11. C.P. Gardiner, R.E. Melchers, *Corros. Sci.*, 44 (2002) 2459-2478.
12. J. Jiang, J. Wang, W. Wang, W. Zhang, *Electrochim. Acta*, 54 (2009) 3623-3629.
13. J.N. Murray, P.J. Moran, *Corrosion*, 45 (1989) 34-43.
14. Beak W C, Kang T, Sohn H J, *Electrochim. Acta*, 46 (2001) 2321-2325.
15. Cáceres L, Vargas T, Parra M. *Electrochim. Acta*, 54 (2009) 7435-7443.
16. Cáceres L, Vargas T, Herrera L, *Corros. Sci.*, 51 (2009) 971-978.
17. Li Y, Wu J, Zhang D, Wang Y, Hou B, *J. Solid State Electrochem.*, 14 (2010) 1667-1673.
18. Y. J. Li, D. Zhang, J. J. Wang, *J. Ocean Univ. China (Oceanic and Coastal Sea Research)*, 9 (2010) 239-243.
19. M. Stratmann, J. Muller, *Corros. Sci.*, 36 (1994) 327-359.
20. Y. Miyata, S. Asakura, *Corros. Sci.*, 44 (2002) 589- 602.
21. A. Q. Fu, X. Tang, Y. F. Cheng, *Corros. Sci.*, 51(2009) 186-190.
22. K. Darowicki, *Corros. Sci.*, 37 (1995) 913-925.
23. F. F. Eliyan, E. Mahdi, A. Alfantazi, *Corros. Sci.*, 58 (2012) 181-191.
24. X. N. Liao, F. H. Cao, A. N. Chen, W. J. Liu, J. Q. Zhang, C. N. Cao, *Tran. Nonferrous. Met. Soc. China*, 22 (2012) 1239-1249.
25. C. N. Cao, J. Q. Zhang, An introduction to electrochemical impedance spectroscopy. Beijing: Science Press, 2002 (in Chinese).
26. M. C. Yan, C. Sun, J. Xu, J. H. Dong, W. Ke, *Corros. Sci.*, 80 (2014) 309-317.
27. M. C. Yan, C. Sun, J. Xu, W. Ke, *Int. J. Electrochem. Sci.*, 10 (2015) 1762- 1776.
28. A. Nazarov, T. Prosek, D. Thierry, *Electrochim. Acta*, 53 (2008) 7531- .
29. A.Q. Fu, Y.F. Cheng , *Corros. Sci.*, 51 (2009) 914-920.
30. C. N. Cao. Principles of Electrochemistry of Corrosion, Third Edition. Beijing: Chemical Industry Press, 2008 (in Chinese).